AGU PUBLICATIONS

JGR

Journal of Geophysical Research: Solid Earth

RESEARCH ARTICLE
10.1002/2015JB012625

Key Points:
- Sound velocity of hcp-Fe and Fe-Ni-Si alloy measured up to 2 Mbar in a diamond anvil cell
- Fe-rich Fe-Ni-Si alloy in the hcp phase displays a relatively high Poisson's ratio
- The multifactored constraint implies that hcp Fe-Ni-Si alloy can be abundant in the inner core

Supporting Information:
- Texts S1–S4, Figures S1–S3, and Tables S1–S3

Correspondence to:
J.-F. Lin,
afu@jsg.utexas.edu

Citation:
Liu, J., J.-F. Lin, A. Alatas, M. Y. Hu, J. Zhao, and L. Dubrovinsky (2016), Seismic parameters of hcp-Fe alloyed with Ni and Si in the Earth's inner core, *J. Geophys. Res. Solid Earth*, *121*, doi:10.1002/2015JB012625.

Received 4 NOV 2015
Accepted 19 JAN 2016
Accepted article online 22 JAN 2016

Seismic parameters of hcp-Fe alloyed with Ni and Si in the Earth's inner core

Jin Liu[1], Jung-Fu Lin[1,2], Ahmet Alatas[3], Michael Y. Hu[3], Jiyong Zhao[3], and Leonid Dubrovinsky[4]

[1]Department of Geological Sciences, Jackson School of Geosciences, University of Texas at Austin, Austin, Texas, USA, [2]Center for High Pressure Science and Advanced Technology Research, Shanghai, China, [3]Advanced Photon Source, Argonne National Laboratory, Argonne, Illinois, USA, [4]Bayerisches Geoinstitut, Universität Bayreuth, Bayreuth, Germany

Abstract Iron alloyed with Ni and Si has been suggested to be a major component of the Earth's inner core. High-pressure results on the combined alloying effects of Ni and Si on seismic parameters of iron are thus essential for establishing satisfactory geophysical and geochemical models of the region. Here we have investigated the compressional (V_P) and shear (Vs) wave velocity-density (ρ) relations, Poisson's ratio (ν), and seismic heterogeneity ratios ($dln\rho/dlnV_P$, $dln\rho/dlnV_S$, and $dlnV_P/dlnV_S$) of hcp-Fe and hcp-$Fe_{86.8}Ni_{8.6}Si_{4.6}$ alloy up to 206 GPa and 136 GPa, respectively, using multiple complementary techniques. Compared with the literature velocity values for hcp-Fe and Fe-Ni-Si alloys, our results show that the combined addition of 9.0 wt % Ni and 2.3 wt % Si slightly increases the V_P but significantly decreases the V_S of hcp-Fe at a given density relevant to the inner core. Such distinct alloying effects on velocities of hcp-Fe produce a high ν of about 0.40 for the alloy at inner core densities, which is approximately 20% higher than that for hcp-Fe. Analysis of the literature high *P-T* results on V_P and V_S of Fe alloyed with light elements shows that high temperature can further enhance the ν of hcp-Fe alloyed with Ni and Si. Most significantly, the derived seismic heterogeneity ratios of this hcp alloy present a better match with global seismic observations. Our results provide a multifactored geophysical constraint on the compositional model of the inner core which is consistent with silicon being a major light element alloyed with Fe and 5 wt % Ni.

1. Introduction

Based on shockwave velocity-density measurements on iron, Francis *Birch* [1952] first found that the Earth's outer core was less dense than pure iron by approximately 10% at relevant pressure and temperature (*P-T*) conditions. Together with geophysical and geochemical evidence, it has been proposed that the Earth's core is primarily constituted of iron alloyed with approximately 5 wt % nickel, together with a certain amount of elements lighter than iron, hereafter named light elements [*Dubrovinsky and Lin*, 2009; *Li and Fei*, 2014]. The exact identity and the amount of light elements in the core remains highly debated, although a number of candidates such as H, C, O, Si, and S have been suggested to exist in the core based on cosmochemical, geochemical, and geophysical arguments [*Hirose et al*., 2013]. Ever since Birch's pioneering research, substantial studies have concentrated on investigating physical and chemical properties of candidate Fe-light element(s) alloys in the binary and ternary systems at relevant *P-T* conditions of the Earth's core including their equation of states, velocity-density profiles, crystal structures, melting curves, solubility in the liquid and solid iron-nickel alloy, as well as partition coefficients between liquid iron and mantle silicates (see reviews by *Dubrovinsky and Lin* [2009] and *Li and Fei* [2014]). These studies have indicated that the liquid outer core contains approximately 6–10 wt % light element(s) while the solid inner core contains approximately 1–4 wt % light element(s) [*Li and Fei*, 2014].

Silicon has been considered as one of the most predominant light elements among the aforementioned candidate elements due to its abundance in the solar system, its preferential partitioning into iron-nickel metal especially under relatively reduced conditions, as well as the velocity-density profile of Fe alloyed with Si that matches seismic observations of the core [e.g., *Gessmann et al*., 2001; *Lin et al*., 2002; *Mao et al*., 2012; *Seagle et al*., 2013; *Siebert et al*., 2013; *Zhang et al*., 2014]. The alloying effects of Si on the structural stability and elasticity of Fe at high *P-T* relevant to the Earth's core are of particular interest in regard to the geophysical constraints on the light elements in the core. Theoretical and experimental results have shown that the incorporation of Si into Fe can enhance the stability field as well as the V_P and V_S anisotropy of Fe in the body-centered cubic (bcc) structure [*Lin et al*., 2002; *Belonoshko et al*., 2003; *Lin et al*., 2003; *Liu et al*., 2014], although Fe with approximately 4–5 wt % Si is likely to be stable in the hexagonal close packed (hcp) structure at relevant *P-T* conditions of the inner core [*Lin et al*., 2002; *Asanuma et al*., 2011; *Tateno et al*., 2015].

Furthermore, hcp-Fe with up to approximately 8 wt % Si exhibits a similar compressional wave velocity and density (V_P-ρ) behavior to that of the hcp-Fe at high pressure, except that there is a decrease in density due to the light element Si substitution in the hcp-Fe lattice [*Mao et al*., 2012]. That is, the main alloying effect of Si on the V_P-ρ of hcp-Fe is a decrease in the density of the alloy due to the lighter mass of the substituting Si. These results further show that the V_P-ρ profile of hcp-Fe with 4–8 wt % Si provides a better match to that of seismological observations in the Earth's inner core.

Since the core likely contains approximately 5 wt % Ni, knowledge of the combined alloying effects of Ni and light element(s) on physical and chemical properties of Fe at the *P-T* conditions of the Earth's core is important for our understanding of the geophysical constraints on the region. Ab initio calculations and high *P-T* synchrotron X-ray diffraction experiments on Fe-Ni alloys have shown that Fe with up to approximately 10 wt % Ni is most likely stable in the hcp structure at the *P-T* conditions of the inner core [*Kamada et al*., 2014]. In terms of the alloying effects of Ni on the elasticity of Fe, previous studies have shown that substitution of Ni into Fe has relatively small effects on the equation of state (EoS) parameters and the V_P-ρ and V_S-ρ of hcp-Fe at high pressure because Ni has relatively similar mass and electronic states to that of Fe [*Mao et al*., 1990; *Lin et al*., 2003; *Martorell et al*., 2013]. These studies also found that Fe with up to 20% Ni has nearly identical EoS parameters as pure Fe up to 300 GPa at 300 K, while the V_P and V_S of hcp-Fe at a given density are slightly reduced by the addition of 8% Ni [*Mao et al*., 1990; *Lin et al*., 2003].

The combined effects of Ni and light element(s) on physical and chemical properties of Fe are of particular interest to our understanding of the geophysics and geochemistry of the Earth's core, because the region is expected to contain not only Fe with approximately 5 wt % Ni but also a certain amount of major as well as minor light elements such that Ni and Si possibly coalloy with Fe in the core. However, other than a handful of studies [*Antonangeli et al*., 2010; *Asanuma et al*., 2011; *Sakai et al*., 2011], the high-pressure compression and sound velocities of Fe-Ni-Si alloys have been relatively unexplored. $Fe_{83}Ni_9Si_8$ and $Fe_{88}Ni_4Si_8$ alloys have been reported to remain in the hcp structure up to 374 GPa at 300 K and 304 GPa at approximately 3000 K, respectively, indicating that the crystal structure is likely to be the hcp structure for Fe alloyed with approximately 4 wt % Si and 9 wt % Ni under inner core conditions [*Asanuma et al*., 2011; *Sakai et al*., 2011]. The V_P-ρ profile of hcp-$Fe_{89}Ni_4Si_7$ alloy measured up to 108 GPa at 300 K suggested an inner core composition containing 4–5 wt % Ni and 1–2 wt % Si [*Antonangeli et al*., 2010], while static compression results for hcp-$Fe_{83}Ni_9Si_8$ alloy, covering the entire pressure conditions of the core, indicated that the inner core would contain approximately 5 wt % Ni and 5 wt % Si [*Asanuma et al*., 2011]. It should be noted that most previous mineral physics studies on the compositional model of the core typically use one seismic parameter (e.g., V_P or density) for comparison with seismic models (e.g., preliminary reference Earth model (PREM)) in order to estimate the amount of a potential light element in the core, leading to major discrepancies in the derived compositions among different studies. The composition of the core can be much better deciphered if multiple seismic parameters, including V_P, V_S, Poisson's ratio, and seismic heterogeneity ratios of hcp Fe-Ni alloyed with a candidate light element are experimentally investigated simultaneously at relevant core conditions.

In this study, multiple seismic parameters of hcp-Fe and $Fe_{86.8}Ni_{8.6}Si_{4.6}$ alloy including the measured sound velocity-density profiles (V_P- and V_S-ρ) and the further derived Poisson's ratio and seismic heterogeneity ratios ($dln\rho/dlnV_P$, $dln\rho/dlnV_S$, and $dlnV_P/dlnV_S$) have been investigated together using high-energy resolution inelastic X-ray scattering (HERIX), nuclear resonant inelastic X-ray scattering (NRIXS), and X-ray diffraction (XRD) spectroscopies in a diamond anvil cell (DAC) up to 206 GPa. Combining with literature values on the velocity-density relations of hcp-Fe alloys, these multiple seismic parameters are jointly used to evaluate the combined alloying effects of Si and Ni on seismic behavior of hcp-Fe which in turn allows us to provide a multifactored geophysical constraint on the compositional model of the Earth's inner core.

2. Experimental Methods

The ^{57}Fe enriched iron (>95% enrichment) powder sample was purchased from Cambridge Isotope Laboratories, Inc. For synthesizing the polycrystalline Fe-Ni-Si alloy (with ^{57}Fe enrichment of >99%), a mixture of powder iron, nickel, and silicon with a starting atomic ratio of 85:10:5 was used for the arc-melting synthesis above 2000 K in an arc furnace in a pure argon atmosphere at Max Planck Institute Stuttgart. Consequently, the ingots were milled and then homogenized in vacuum at 900°C for approximately 5 days at the Bayerisches Geoinstitut. Electron microprobe analyses showed that the alloy was chemically homogeneous and had a chemical composition of

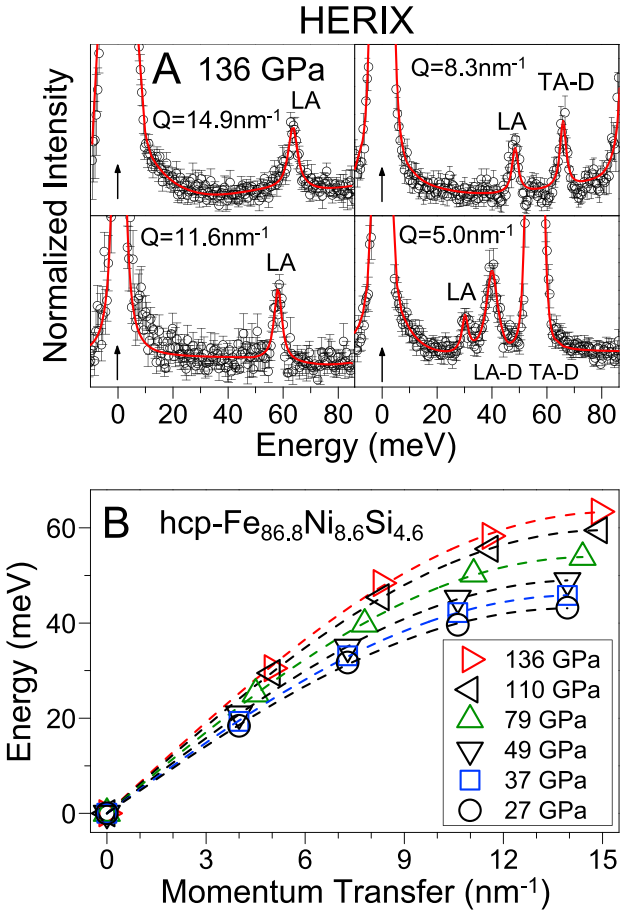

Figure 1. HERIX spectra and phonon dispersion curves of hcp-$Fe_{86.8}Ni_{8.6}Si_{4.6}$ alloy at high pressure. (a) Representative HERIX spectra as a function of momentum transfer (Q) at 136 GPa. (b) The longitudinal acoustic phonon dispersion curves of hcp-$Fe_{86.8}Ni_{8.6}Si_{4.6}$ alloy as a function of pressure. Open circles with error bars: HERIX experimental data and solid lines: fits with a Lorentzian function for the longitudinal acoustic phonon peak (LA). The up arrow denotes the elastic peak at zero energy position. Transverse acoustic (TA-D) and longitudinal acoustic (LA-D) phonon peaks from the diamond anvils were also recorded at the momentum transfers (Q) of 5.0 and 8.3 nm^{-1}, respectively. Note that the elastic peaks at zero energy position are not fully shown in order to avoid the elastic peak dominating the plot since the intensity of elastic peaks is typically 20–40 times higher than that of the acoustic phonon peak of the alloy [*Liu et al.*, 2014]. The measured momentum-energy (Q-E) relations (open symbols) from the HERIX spectra were fitted using a sine function (dashed lines), in which the Q-E transfers at the origin of the first Brillouin zone are intrinsically set at zero for the data analyses. The uncertainty of the momentum transfer (Q) is 0.30–0.35 nm^{-1}. Errors ($\pm 1\sigma$) of the energy transfer (E) are typically less than 1%. Error bars smaller than the symbols are not shown for clarity.

$Fe_{86.8}Ni_{8.6}Si_{4.6}$ containing 9.0 (±0.1) wt % Ni and 2.3 (±0.1) wt % Si, which is slightly different from the starting composition likely due to the more loss of Ni and Si during the arc-melting process; other impurities such as oxygen were below the detection limit of the technique. XRD patterns showed that the alloy was in the bcc structure with lattice parameter $a = 2.8695$ (±0.0009) Å at ambient conditions. For high-pressure X-ray diffraction experiments, an alloy sample of approximately 35 μm in diameter and 10 μm thick was loaded into the sample chamber of 90 μm in diameter and 25 μm thick in a DAC, which was drilled in the center of a Re gasket of 250 μm thick, together with micron-sized Pt powder as the pressure calibrant [*Fei et al.*, 2007]. Ultrapure Ne pressure-transmitting medium was loaded using the high-pressure gas loading system in the Mineral Physics Laboratory of the University of Texas at Austin. XRD measurements were conducted using a highly monochromatized incident X-ray beam with an energy of 37.08 keV (0.3344 Å) and 30.82 keV (0.4024 Å) at the High Pressure Collaborative Access Team (HPCAT) and GeoSoilEnviroConsortium for Advanced Radiation Sources (GSECARS) of the Advanced Photon Source (APS), Argonne National Laboratory (ANL), respectively. The X-ray beam was focused down to a beam size of ~5 μm in diameter (full width at half maximum) at the sample position, and the diffraction patterns were collected by a MAR CCD detector. Diffraction patterns were integrated using the Fit2D program to derive the unit cell parameters of the Fe-Ni-Si sample and Pt pressure calibrant. Pressures and their uncertainties were calculated from the Pt pressure calibrant using a third-order Birch-Murnaghan EoS and standard error propagation procedures [*Fei et al.*, 2007]. Note that the EoS of pressure medium Ne was not systematically cross checked with Pt pressure calibrant in this study due to the spotty and intensity saturation of Ne diffraction peaks at high pressures.

High-pressure HERIX measurements were conducted using a highly monochromatized incident X-ray beam with an energy of 21.657 keV (0.5725 Å), an energy bandwidth of 1.15 meV with an overall spectrometer (analyzer and high-resolution monochromator) resolution of 2.1 meV and a beam size of 15–20 μm at the

Table 1. Compressional Wave Velocity of hcp-$Fe_{86.8}Ni_{8.6}Si_{4.6}$ From High-Pressure HERIX Measurements[a]

P (GPa)[b]	ρ (g/cm^3)[c]	V_P (km/s)[d]	Q_{max} (nm^{-1})[e]
27 (±1)	9.22 (±0.01)	7.29 (±0.08)	14.2 (±0.2)
37 (±1)	9.53 (±0.01)	7.68 (±0.09)	14.3 (±0.2)
49 (±1)	9.86 (±0.01)	8.15 (±0.09)	14.4 (±0.2)
79 (±2)	10.54 (±0.01)	8.82 (±0.13)	14.8 (±0.2)
110 (±2)	11.12 (±0.02)	9.41 (±0.11)	15.2 (±0.2)
136 (±2)	11.55 (±0.02)	9.89 (±0.16)	15.3 (±0.3)

[a]Neon was used as the pressure-transmitting medium. Pressures were calculated from the equation of state (EoS) of the alloy itself in this study.
[b]Pressure was calculated from the equation of state (EoS) of the alloy itself in this study.
[c]Density (ρ) was for the ^{57}Fe-enriched alloy, which was calculated from analyzing unit cell parameters from X-ray diffraction patterns collected during the HERIX measurements, after considering the sample composition of 99% ^{57}Fe-enrichment in the alloy. Density for the naturally isotopic composition (with 2% ^{57}Fe) shall be converted by dividing a factor of 1.018 for the alloy.
[d]The compressional wave velocity (V_P) was for the ^{57}Fe-enriched sample. The V_P for the naturally isotopic composition (with 2% ^{57}Fe) shall be converted by multiplying a factor of 1.009 for the alloy.
[e]Q_{max} was considered as a free parameter when fitting the measured phonon dispersion curve to a sine function of the momentum and energy transfers (see supporting information for more details).

3IDC of the APS, ANL (see *Alatas et al.* [2011], *Toellner et al.* [2011], and *Mao et al.* [2012] for more details). A Re gasket of 250 μm thick was preindented to ~25 μm thick by a pair of diamond anvils with 150–300 μm beveled culets, and a hole of 90 μm in diameter was then drilled in the center. A powder sample of ~30 μm in diameter and ~15 μm in thickness was then loaded into the sample chamber with Ne as the pressure transmitting medium; the use of the pressure medium and a small sample size helped to reduce potential gradients in the measurements. In order to have the transverse acoustic peak of the diamond anvils at a higher energy to avoid potential peak overlapping with the sample longitudinal acoustic peak and to achieve a lower diamond background noise close to the sample longitudinal acoustic peaks, the diamond anvils were preoriented with fast velocity direction aligned along the momentum transfer. The collection time for each energy scan was approximately 1.5 h, and about 20 spectra were added together for each given pressure in order to obtain high-quality HERIX spectra of the samples. The density of the sample and its uncertainty were calculated from X-ray diffraction patterns taken during the HERIX measurements and were then used to calculate the pressure of the sample using the EoS calibrated against the Pt scale in this study using XRD. The pressure uncertainty was determined from XRD patterns collected

Table 2. Sound Velocities of hcp-Fe and $Fe_{86.8}Ni_{8.6}Si_{4.6}$ From High-Pressure NRIXS Measurements

P (GPa)[a]	Energy Range (meV)[c]	ρ (g/cm^3)[d]	V_D (km/s)[e]	V_S (km/s)[f]
		hcp-$Fe_{86.8}Ni_{8.6}Si_{4.6}$		
30 (±1)	3.5–13.0	9.34 (±0.01)	3.89 (±0.02)	3.45 (±0.02)
44 (±1)	3.5–12.5	9.72 (±0.01)	4.08 (±0.04)	3.62 (±0.04)
57 (±1)	3.5–13.5	10.06 (±0.01)	4.21 (±0.04)	3.73 (±0.04)
83 (±2)	3.5–15.2	10.62 (±0.02)	4.48 (±0.05)	3.97 (±0.04)
106 (±2)	3.5–16.0	11.05 (±0.02)	4.61 (±0.03)	4.08 (±0.03)
133 (±2)	3.5–16.5	11.50 (±0.03)	4.75 (±0.05)	4.20 (±0.05)
		hcp-Fe		
145 (±3)[b]	4.0–17.8	12.04 (±0.05)	5.58 (±0.05)	4.97 (±0.07)
182 (±5)[b]	4.0–17.3	12.58 (±0.07)	5.80 (±0.05)	5.17 (±0.07)
206 (±6)[b]	4.0–18.5	12.90 (±0.07)	5.94 (±0.05)	5.29 (±0.07)

[a]Pressure for the alloy was calculated from the equation of state (EoS) of the alloy itself in this study; pressure for hcp-Fe was calculated from the EoS of hcp-Fe reported by *Dewaele et al.* [2006].
[b]NaCl was used as the pressure-transmitting medium for NRIXS measurements on hcp-Fe. For the alloy, neon used as the pressure-transmitting medium.
[c]The energy range was used to derive the Debye sound velocity (V_D) by the best fit of the PDOS according to χ^2 analysis.
[d]Density (ρ) for the ^{57}Fe-enriched samples was calculated from analyzing unit cell parameters from X-ray diffraction patterns collected during the NRIXS measurements, after considering the sample composition of 95% and 99% ^{57}Fe-enrichment for hcp-Fe and $Fe_{86.8}Ni_{8.6}Si_{4.6}$ alloy, respectively. Density for the naturally isotopic composition (with 2% ^{57}Fe) shall be converted by dividing a factor of 1.018 for the alloy and 1.020 for hcp-Fe.
[e]The Debye sound velocity (V_D) was for the ^{57}Fe-enriched sample. The V_D for the naturally isotopic composition (with 2% ^{57}Fe) shall be converted by multiplying a factor of 1.009 for the alloy and 1.010 for hcp-Fe.
[f]The shear wave velocity (V_S) for the ^{57}Fe-enriched sample was calculated from the NRIXS and HERIX measurements, independently from the EoS (see supporting information for more details).

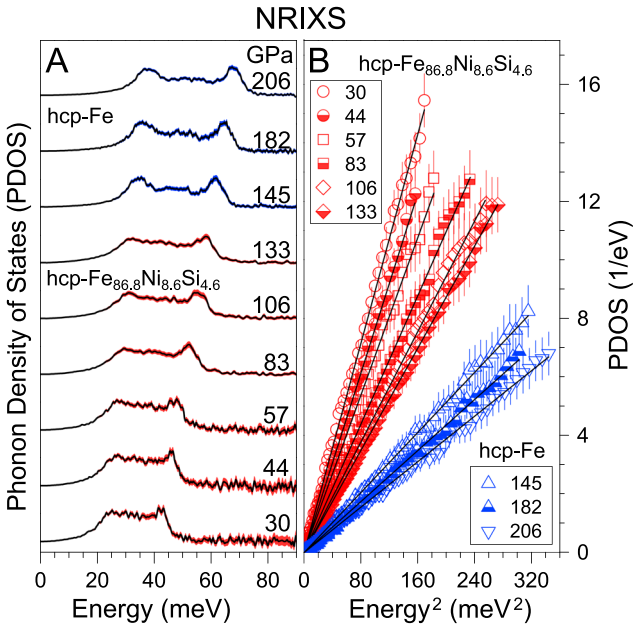

Figure 2. Phonon density of states and the derivation of V_D of hcp-Fe and hcp-$Fe_{86.8}Ni_{8.6}Si_{4.6}$ alloy from high-pressure NRIXS measurements. (a) Phonon density of states (PDOS) of hcp-Fe and hcp-$Fe_{86.8}Ni_{8.6}Si_{4.6}$ alloy as a function of pressure. (b) Low-energy portions of the PDOS of hcp-Fe and hcp-$Fe_{86.8}Ni_{8.6}Si_{4.6}$ alloy as a function of the energy squared. Red and blue margins represent uncertainties of the PDOS of hcp-Fe and hcp-$Fe_{86.8}Ni_{8.6}Si_{4.6}$ alloy, respectively. The solid lines represent the best linear fits of the PDOS versus the energy squared (open symbols), from which Debye velocities are derived according to χ^2 analysis.

before and after the HERIX measurements and included the propagated uncertainty from the EoS reported in this study. Based on the analyses of the diffraction patterns of the alloy up to 136 GPa, the sample slightly developed some textures, but the degree of texturing did not resemble those of hcp-Fe in nonhydrostatic conditions [*Wenk et al.*, 2000] (Figure S2 in the supporting information). Therefore, the velocity reported here is treated as the aggregate V_P of the polycrystalline hcp-$Fe_{86.8}Ni_{8.6}Si_{4.6}$ alloy.

For high-pressure NRIXS measurements, a threefold panoramic DAC was used to increase the detection area and thus enhance the detecting efficiency of the fluorescence signal [*Mao et al.*, 2001]. A Be gasket with a cubic boron nitride (cBN) gasket insert was employed to permit a thicker sample chamber as well as higher pressure measurements (see *Lin et al.* [2010] for more details). The cBN insert in the Be gasket was preindented to 25 GPa (approximately 25–30 μm thick) using a pair of diamond anvils with culets of 150 μm in diameter. Consequently, a 90 μm diameter hole was drilled in the center of the preindentation using a mechanical drilling machine in the Mineral Physics Laboratory of the University of Texas at Austin. The alloy sample of ~15 μm thick and ~30 μm in diameter was loaded into the sample chamber together with a ruby sphere of <5 μm. Ultrapure neon was then loaded into the sample chamber as the pressure transmitting medium. For NRIXS measurements on hcp-Fe, an iron sample disk of <10 μm thick and ~15 μm in diameter was loaded into the sample chamber along with a pair of beveled diamond anvils having the culet size of 60-180-300 μm (or 50–300 μm). Two layers of dry NaCl of ~1 μm thick were placed on each side of sample at the center of the diamond culets and used as the pressure medium. Similar to HERIX experiments, the density of the sample was taken from analyses of the XRD patterns, while the pressure of the sample was calculated based on the EoS and XRD patterns of the sample. NRIXS experiments were performed at 3IDB of the APS, ANL. The incident X-ray beam with a bandwidth of 1.2 meV (energy resolution) was focused by a Kirkpatrick-Baez mirror system to a beam size of ~10 μm by 10 μm at the sample position [*Zhao et al.*, 2004]. The NRIXS energy spectrum was obtained by tuning the incident X-ray energy approximately from −90 to +110 meV for the alloy and −110 to +150 meV for hcp-Fe around the ^{57}Fe nuclear transition energy at 14.4125 keV with a step size of 0.25 meV and a collection time of 5 s per energy step. Fifteen to 40 spectra per pressure were collected in order to achieve good statistics for the data.

3. Results

XRD patterns of the hcp-$Fe_{86.8}Ni_{8.6}Si_{4.6}$ alloy were collected at pressures up to 147 GPa and 300 K (Figure S1). The compression curve of the alloy shows a volume reduction of ~4% across the phase transition from the bcc to hcp phase around 16–20 GPa, consistent with that reported for $Fe_{83}Ni_9Si_8$ alloy by *Asanuma et al.* [2011] (Tables S1 and S2). Comparison of the *P-V* curves between hcp-Fe and the alloy indicates that the combined effects of Ni and Si on the compression curve of the hcp-Fe under core pressures are negligible [*Asanuma et al.*, 2011]. Furthermore, the axial ratio (*c*/*a*) of the sample is approximately 1.60 at pressures from approximately 70 GPa to 147 GPa (Figure S1 insert).

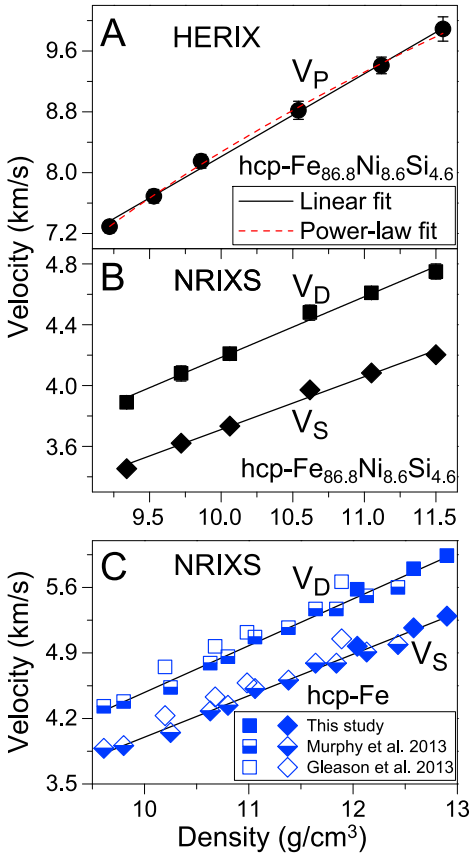

Figure 3. Sound velocities of ^{57}Fe-enriched hcp-Fe and hcp-$Fe_{86.8}Ni_{8.6}Si_{4.6}$ alloy as a function of density. (a) V_P of hcp-$Fe_{86.8}Ni_{8.6}Si_{4.6}$ alloy derived from HERIX measurements. (b) V_D and V_S of hcp-$Fe_{86.8}Ni_{8.6}Si_{4.6}$ alloy derived from NRIXS measurements. (c) V_D and V_S of hcp-Fe derived from NRIXS measurements. V_S reported in this study was calculated from the V_P and V_D. The density in this figure is calculated by considering 95% and 99% ^{57}Fe-enrichment in the Fe and $Fe_{86.8}Ni_{8.6}Si_{4.6}$ alloy, respectively. Black and blue solid symbols: hcp-$Fe_{86.8}Ni_{8.6}Si_{4.6}$ and hcp-Fe, respectively (this study); half-filled symbols: hcp-Fe [*Murphy et al.*, 2013]; open symbols: hcp-Fe [*Gleason et al.*, 2013]; solid lines: linear fits; dashed line: power law fit; and vertical ticks: representative errors ($\pm 1\sigma$) calculated using standard error propagations. Error bars smaller than the symbols are not shown for clarity.

HERIX spectra of the alloy at momentum transfers (Q) from 4.0 to 14.9 nm^{-1} were collected from the hcp-$Fe_{86.8}Ni_{8.6}Si_{4.6}$ at six given pressures of 27, 37, 49, 79, 110, and 136 GPa (Figure 1 and Table 1). The energy spectra were fitted to a Lorentzian function using the OriginPro 9.0 software to derive the energy of the longitudinal acoustic (LA) phonon peak (E) of the alloy and the transverse acoustic (TA) phonon peak of the diamond anvils (Figure 1). The V_P of the hcp-$Fe_{86.8}Ni_{8.6}Si_{4.6}$ was then derived from fitting the measured LA phonon dispersion curve to a sine function of the momentum (Q) and energy transfers (E) (see *Fiquet et al.* [2001] and supporting information for further details). Together with the density of the sample from complementary in situ XRD measurements, the derived V_P-ρ profile of the alloy up to 136 GPa can be fitted to a power law function and a linear regression function within the statistical uncertainties of the experimental data (Figure 3*a*) (see supporting information for more details). Both the power law and linear fitting results were reported in the present study for comparison with literature results.

NRIXS spectra were collected at ambient conditions and at 6, 17, 30, 44, 57, 83, 106, and 133 GPa for the ^{57}Fe-enriched hcp-$Fe_{86.8}Ni_{8.6}Si_{4.6}$ and at 145, 182, and 206 GPa for hcp-Fe (Tables 2 and S3). The measured NRIXS spectra were processed using the PHOENIX program (Version 2.1.1) via removing the elastic contribution and applying the quasi harmonic lattice model to extract the partial phonon density of states (PDOS) of the ^{57}Fe isotope in the aggregate hcp-$Fe_{86.8}Ni_{8.6}Si_{4.6}$ alloy and the full PDOS of the aggregate hcp-Fe [*Sturhahn*, 2000] (Figure 2a). The low-energy portion of the PDOS can be used to derive the Debye sound velocity (V_D) using the Debye model [*Sturhahn*, 2000] (Figure 2b). The low-energy range of the PDOS was determined using the best fit in the χ^2 analysis and then used to derive V_D. Together with the density from in situ XRD measurements, the V_D-ρ profile of hcp-$Fe_{86.8}Ni_{8.6}Si_{4.6}$ from 30 to 133 GPa can be well fitted using a linear function within statistical uncertainties (Figure 3b). We note that *Gleason et al.* [2013] pointed out the sound velocity of hcp-Fe measured by NRIXS measurements relatively higher under hydrostatic than nonhydrostatic conditions. In particular, *Murphy et al.* [2013] and *Gleason et al.* [2013] reported the V_D of hcp-Fe was 4.79 (±0.04) at 69 GPa and 4.97 (±0.02) at 71 GPa, respectively. Both V_D values were derived from the PDOS spectra measured at the same beamline using neon as the pressure-transmitting medium. The difference in V_D is approximately 4% at 69–71 GPa between these two studies, likely due to the minimum energy of 1.7 meV fitted in *Gleason et al.* [2013] which marginally fell within the width of the measured resolution functions. We found that the new V_D data of hcp-Fe between 145 and 206 GPa could be fairly combined with the literature results by *Murphy et al.* [2013]. The combined data set is fairly well represented by a linear function (Figure 3*c*) (see supporting information for more details).

Since the sound velocities derived from NRIXS and HERIX measurements could represent an aggregate sample in this study, it is reasonable to combine these two experimental techniques to derive the V_S of the polycrystalline

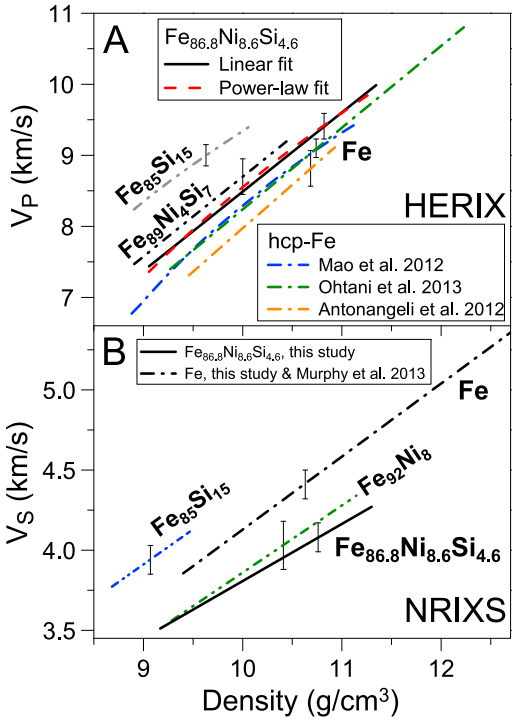

Figure 4. Sound velocity and density relations of hcp-Fe and Fe-Ni-Si alloys at high pressure. (a) Compressive wave velocity (V_P) derived from HERIX measurements. (b) Shear wave velocity (V_S) derived from NRIXS measurements. The reported sound velocity and density were converted from the corresponding ^{57}Fe-enriched sample for Fe atoms with a natural ^{57}Fe isotope concentration of 2% (see Tables 1 and 2 for more details). Black solid lines: linear fits for hcp-$Fe_{86.8}Ni_{8.6}Si_{4.6}$ alloy (this study); red dashed line: a power law fit for hcp-$Fe_{86.8}Ni_{8.6}Si_{4.6}$ alloy (this study); black dash-dotted line: V_S of hcp-Fe (this study) [*Murphy et al.*, 2013]; blue, olive, and orange dash-dotted lines: V_P of hcp-Fe from HERIX measurements [*Antonangeli et al.*, 2012; *Mao et al.*, 2012; *Ohtani et al.*, 2013]; black dash-dot-dotted line: V_P of hcp-$Fe_{89}Ni_4Si_7$ [*Antonangeli et al.*, 2010]; gray dash-dot-dotted line: V_P of hcp-$Fe_{85}Si_{15}$ [*Mao et al.*, 2012]; blue and olive dash-dot-dotted lines: V_S of hcp-$Fe_{85}Si_{15}$ and hcp-$Fe_{92}Ni_8$ alloys, respectively [*Lin et al.*, 2003]; and vertical ticks: representative errors ($\pm 1\sigma$) calculated using standard error propagations.

iron and iron-alloy at high pressure; however, readers should be aware of that the energies and polarization of the phonons probed by NRIXS measurements are not the same as HERIX measurements. We have also calculated V_S and Poisson's ratio (ν) of the sample from V_P in HERIX measurements and V_D in NRIXS measurements using equations (S5) and (S6) in the supporting information. The derived V_S-ρ profiles of hcp-Fe and the alloy were then fitted by a linear function (see supporting information for fitting parameters).

The difference in the sound velocity-density relation between the ^{57}Fe-enriched sample and Fe with a natural isotopic ratio should not be neglected. When comparing experimental results with seismological observations (e.g., PREM) for geophysical implications, the relation should be corrected for Fe or Fe alloys with a natural Fe isotopic ratio. The polycrystalline samples used for our high-pressure experiments are all enriched in the heavier isotope of ^{57}Fe and have a relatively higher density and a lower velocity than the corresponding samples with a natural ^{57}Fe-content of approximately 2%. With the assumption that the elastic modulus and the unit cell volume are independent of the isotopic mass, the sound velocity of the ^{57}Fe-enriched samples $\left(V_{P,S,D}^{\mathrm{Enrich}}\right)$ was converted for that of the corresponding natural ^{57}Fe-content samples $\left(V_{P,S,D}^{\mathrm{Natl}}\right)$ using the following relation [*Sturhahn and Jackson*, 2007; *Gao et al.*, 2011]:

$$V_{P,S,D}^{\mathrm{Natl}} = V_{P,S,D}^{\mathrm{Enrich}} \sqrt{M^{\mathrm{Enrich}}/M^{\mathrm{Natl}}},$$

where M^{Enrich} and M^{Natl} represent the atomic mass of the ^{57}Fe-enriched and natural samples, respectively, and the subscripted P, S, and D represent compressional, shear, and Debye sound velocity, respectively. For the 95% ^{57}Fe-enriched hcp-Fe sample, $M^{\mathrm{Enrich}} = 56.95$ g/mol and $M^{\mathrm{Natl}} = 55.85$ g/mol are used in the conversion, resulting in approximately −2.0% correction for density and +1.0% correction for velocity of the natural composition. For the 99% ^{57}Fe-enriched $Fe_{86.8}Ni_{8.6}Si_{4.6}$ alloy, the alloy has $M^{\mathrm{Enrich}} = 55.77$ g/mol and $M^{\mathrm{Natl}} = 54.81$ g/mol, resulting in approximately −1.8% and +0.9% corrections for the density and sound velocity of the natural composition, respectively. The fitting parameters for the velocity-density profiles of the ^{57}Fe-enriched and naturally isotopic samples are provided in the supporting information.

4. Discussion and Implications

4.1. Combined Alloying Effects of Ni and Si on the V_P-ρ and V_S-ρ Profiles of hcp-Fe

Comparison of seismic observations of the Earth's core and the pressure-velocity-density relations of candidate Fe-rich alloys provides one of the most accepted geophysical means to constrain the type and the amount of potential light elements needed to compensate the sound velocity and density deficit in the core [*Badro et al.*, 2007]. It is worthwhile to note that many experimental techniques have been used to explore

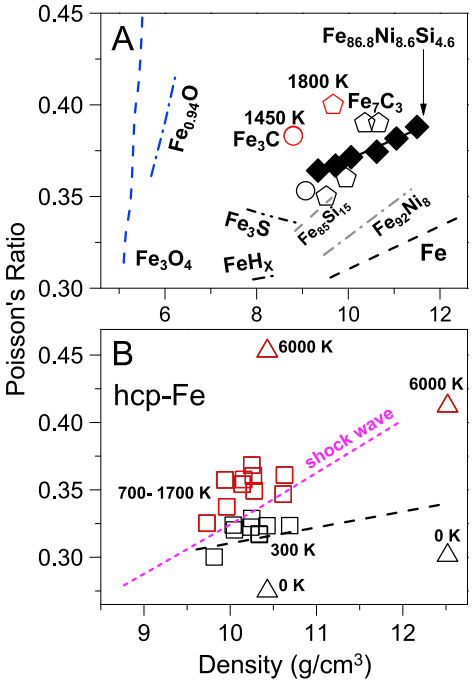

Figure 5. Poisson's ratio of hcp-Fe and Fe-rich alloys as a function of density. Temperatures are labeled next to the symbols to specify temperature conditions, while the ones without temperatures labeled are under ambient temperature. Solid line and diamonds: hcp-$Fe_{86.8}Ni_{8.6}Si_{4.6}$ at 300 K (this study); black dashed line: hcp-Fe at 300 K [this study; *Murphy et al.*, 2013]; gray dashed and dash-dotted lines: hcp-$Fe_{85}Si_{15}$ and hcp-$Fe_{92}Ni_8$ alloys at 300 K, respectively [*Lin et al.*, 2003]; black dash-dotted line: Fe-H alloy at 300 K [*Mao et al.*, 2004; *Shibazaki et al.*, 2012]; black dash-dot-dotted line: Fe_3S at 300 K [*Lin et al.*, 2004; *Kamada et al.*, 2014]; black and red pentagons: the low-spin orthorhombic Fe_7C_3 at 300 K and 1800 K, respectively [*Prescher et al.*, 2015]; black and red circles: orthorhombic Fe_3C at 300 K and 1450 K, respectively [*Gao et al.*, 2011]; black and red squares: hcp-Fe at 300 K and 700–1700 K, respectively [*Lin et al.*, 2005]; magenta short-dashed line: hcp-Fe along the Hugoniot from shock wave experiments [*Duffy and Ahrens*, 1992]; black and red triangles: theoretical calculations, hcp-Fe at 0 K and 6000 K, respectively [*Sha and Cohen*, 2010]; blue dashed line: Fe_3O_4-magnetite at 300 K and 0–20 GPa [*Lin et al.*, 2014]; and blue dash-dotted line: $Fe_{0.94}O$-wüstite at 300 K and 0–16 GPa [*Kantor et al.*, 2004]. Note that the theoretical values of the Poisson's ratio were calculated from single-crystal elastic constants of hcp-Fe reported by *Sha and Cohen* [2010] using the Voigt-Reuss-Hill average method by *Hill* [1952].

the sound velocities of iron and its alloys at high pressure and/or high temperature, including the pulse-echo ultrasonics, picosecond acoustics, impulsive stimulated light scattering, shock compression, and inelastic X-ray scattering [e.g., *Mao et al.*, 1998; *Fiquet et al.*, 2001; *Mao et al.*, 2001; *Nguyen and Holmes*, 2004; *Decremps et al.*, 2014]. To date, results from most previous studies are not all in agreement on the absolute velocity value and pressure-density-velocity relation of hcp-Fe, likely due to their differences in the technical aspects (see *Antonangeli and Ohtani* [2015] for a recent review). Therefore, a more consistent comparison could be made using results derived from the same techniques. To understand the combined alloying effects of Ni and Si on the sound velocity of hcp-Fe, here we have systematically examined the high-pressure HERIX or NRIXS measurements for the velocities of hcp-Fe, Fe-Si, Fe-Ni, and Fe-Ni-Si alloys (Figure 4) [*Lin et al.*, 2003; *Antonangeli et al.*, 2010; *Antonangeli et al.*, 2012; *Mao et al.*, 2012; *Murphy et al.*, 2013; *Ohtani et al.*, 2013].

Compared to pure Fe, hcp-$Fe_{86.8}Ni_{8.6}Si_{4.6}$ alloy exhibits a higher V_P-ρ profile but with a similar curvature (Figure 4a). The hcp-$Fe_{89}Ni_4Si_7$ alloy in a previous study displays a slightly higher V_P-ρ profile than the alloy in this study, due to the addition of more silicon and less nickel [*Antonangeli et al.*, 2010]. Based on HERIX results, the V_P of hcp-Fe at a constant density of 10 g/cm^3 increases by 0.081 (±0.009) km/s by adding 1 mol% Si, but the addition of 1 mol% Ni decreases the value by approximately 0.005 km/s. That is, nickel has a negligible effect on the V_P of Fe-Ni-Si alloys, consistent with previous studies on the hcp-$Fe_{92}Ni_8$ alloy [*Lin et al.*, 2003]. On the other hand, the combined alloying effect of Ni-Si on the V_S is different from that on the V_P of hcp-Fe. Compared to hcp-Fe, the hcp-$Fe_{86.8}Ni_{8.6}Si_{4.6}$ alloy exhibits a lower V_S-ρ profile (Figure 4b). The V_S-ρ profiles of the Fe-rich Fe-Ni and Fe-Ni-Si alloys are lower than that of hcp-Fe, while the Fe-Si alloy displays a higher V_S-ρ profile than hcp-Fe. According to high-pressure NRIXS results, the V_S of hcp-Fe at a constant density of 10 g/cm^3 is modified by +0.012 (±0.002) km/s and −0.039 (±0.005) km/s with the addition of 1 mol% Si and Ni, respectively. In contrast to the combined effect on V_P, Ni has a greater effect on V_S than Si in the hcp Fe-rich Fe-Ni-Si alloy. It should be noted that theoretical calculations found that the addition of Ni strongly reduces the V_S of hcp-Fe via the significant reduction in c_{44} at relatively low temperature [*Martorell et al.*, 2013]. The V_S reduction in the Fe-rich Fe-Ni-Si alloy caused by the Ni addition may help explain the large discrepancy in the V_S between hcp-Fe and the inner core [e.g., *Steinle-Neumann et al.*, 2001; *Lin et al.*, 2005; *Sha and Cohen*, 2010; *Gao et al.*, 2011].

4.2. Light Element Alloying Effects on the Poisson's Ratio of hcp-Fe

The Poisson's ratio (ν) of the Earth's inner core from seismic observations can also be used as a geophysical constraint on the composition of the region [*Prescher et al.*, 2015]. According to seismological observations

(e.g., PREM), the Poisson's ratio of the inner core ranges from approximate 0.444 to 0.441, while the Poisson's ratio of hcp-Fe at 300 K is about 0.33–0.34 at given densities relevant to the inner core in the present study [*Mao et al*., 2001; *Murphy et al*., 2013]. Such large divergence for ν between the inner core and hcp-Fe at 300 K implies two possibilities: (a) the existence of candidate light element(s) would greatly enhance the Poisson's ratio being closer to the inner core value and (b) high-temperature effect on the ν of hcp-Fe and Fe-rich alloys can be significant and cannot be neglected. Since the Poisson's ratio represents an expression of the V_P/V_S ratio, it is conceivable that the V_P and V_S of a given Fe-rich alloy can respond to the alloying and/or high-temperature effects differently. Here we have examined the Poisson's ratio of hcp-Fe and Fe alloys in order to evaluate potential alloying effects (Figure 5) [*Duffy and Ahrens*, 1992; *Lin et al*., 2003; *Kantor et al*., 2004; *Lin et al*., 2004; *Mao et al*., 2004; *Lin et al*., 2005; *Sha and Cohen*, 2010; *Gao et al*., 2011; *Shibazaki et al*., 2012; *Murphy et al*., 2013; *Kamada et al*., 2014; *Lin et al*., 2014; *Prescher et al*., 2015]. Analysis of these results of the alloying effects on the ν of hcp-Fe shows that at a given density, H has negligible alloying effects, S and Si individually enhance the ν of hcp-Fe, and C and O cause the Poisson's ratio to increase drastically (Figure 5a). Among all candidate light element compounds investigated at high pressures and room temperature, Fe_7C_3 compound has a very high ν value at core pressures, which has been used as an argument for carbon being a major light element component in the Earth's core [*Prescher et al*., 2015]. Fe_7C_3 exhibits the anomalously low V_S at core pressures, which in turn raises up the values of V_P/V_S and ν. This anomalously low V_S is proposed to be caused by the shear softening associated with a pressure-induced spin-pairing transition of iron in Fe_7C_3 [*Chen et al*., 2014]. We note that iron oxides (Fe_3O_4 magnetite and $Fe_{0.94}O$ wüstite) exhibit extremely high Poisson's ratios at pressures of less than 20 GPa largely due to the pressure-induced mode softening of the C_{44} elastic constant [*Kantor et al*., 2004; *Lin et al*., 2014]. Based on our study, the ν of hcp-$Fe_{86.8}Ni_{8.6}Si_{4.6}$ alloy is comparable to the Fe_7C_3 under core pressures at 300 K as a result of the enhanced V_P due to Si addition and the reduced V_S via Ni alloying (Figure 5a).

4.3. High-Temperature Effects on the V_P, V_S, and υ of hcp-Fe and Fe Alloys

Temperature-dependent sound velocity of hcp-Fe and its alloys have been studied theoretically and experimentally [e.g., *Steinle-Neumann et al*., 2001; *Lin et al*., 2005; *Vočadlo et al*., 2009; *Sha and Cohen*, 2010; *Gao et al*., 2011; *Antonangeli et al*., 2012; *Mao et al*., 2012; *Ohtani et al*., 2013]. Early first-principle calculations on the elasticity of hcp-Fe at high temperatures indicated that the V_P of hcp-Fe decreases by 3% from 0 K to 6000 K at a given inner core density of 13.04 g/cm^3 [*Steinle-Neumann et al*., 2001], but more recent first-principle calculations by *Sha and Cohen* [2010] suggested that the V_P of hcp-Fe decreases by 9–10% from 0 K to 6000 K at 10.43 and 12.52 g/cm^3. *Mao et al*. [2012] modeled the combined data sets of hcp-Fe from shockwave and high *P-T* HERIX measurements and found a decrease of approximately 2% in the V_P of hcp-Fe from 300 K to 6000 K at given inner core densities. These results suggested that the temperature dependency on V_P of hcp-Fe is significant at moderate pressures but becomes weaker under inner core pressures. On the other hand, *Ohtani et al*. [2013] observed a small temperature dependence on V_P of hcp-Fe up to 1000 K from high *P-T* HERIX measurements, while *Antonangeli et al*. [2012] proposed that the high-temperature anharmonic corrections on V_P of hcp-Fe are negligible at least up to 1100 K.

High-temperature effect on V_S has been theoretically and experimentally observed to be much stronger than the effect on V_P [e.g., *Steinle-Neumann et al*., 2001; *Lin et al*., 2005; *Sha and Cohen*, 2010; *Gao et al*., 2011]. First-principle calculations suggested the V_S of hcp-Fe decreases by approximately 53%, 36%, 37%, and 27% from 0 to 6000 K at 10.43, 12.52, 13.04, and 15.65 g/cm^3, respectively [*Steinle-Neumann et al*., 2001; *Sha and Cohen*, 2010]. Similarly, *Lin et al*. [2005] and *Gao et al*. [2011] reported that the V_S of hcp-Fe and Fe_3C showed a strong temperature dependence up to 1700 K and 1450 K at moderate high pressures, respectively, from the laser-heated NRIXS measurements. Therefore, the high-temperature effects on sound velocity should be considered when comparing the sound velocity-density profiles of iron-rich alloys with seismic observations to determine the species and quantity of light element(s) in iron.

Here we have systematically analyzed Poisson's ratios of hcp-Fe and its alloys based on literature theoretical and experimental results in order to simultaneously evaluate high *P-T* effects on V_P as well as V_S because the Poisson's ratio reflects the V_P/V_S ratio. This ratio has been reported to increase with increasing temperature for hcp-Fe and Fe-rich alloys, although such a temperature effect has been neglected in studies supporting or arguing against light element(s) in the inner core [e.g., *Duffy and Ahrens*, 1992; *Lin et al*., 2005; *Sha and Cohen*, 2010;

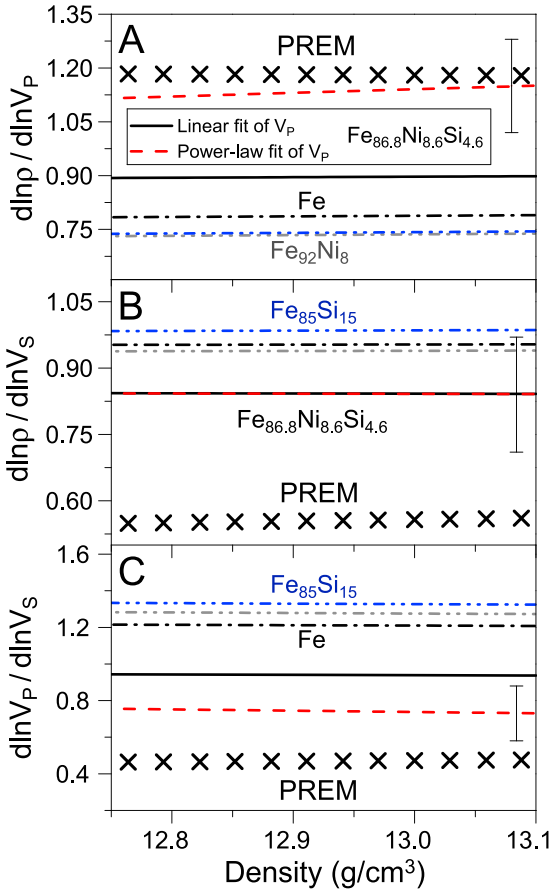

Figure 6. Modeled seismic heterogeneity ratios of hcp-Fe and Fe-Ni-Si alloys as a function of density at 300 K. The density range corresponds to that in the Earth's inner core. (a) The ratio $R_{\rho/P}$ of density to compressional velocity anomaly ($d\ln\rho/d\ln V_P$). (b) The ratio $R_{\rho/S}$ of density to shear velocity anomaly ($d\ln\rho/d\ln V_S$). (c) The ratio $R_{P/S}$ of compressional to shear velocity anomaly ($d\ln V_P/d\ln V_S$). Black solid and red dashed lines: linear and power law fits of hcp-$Fe_{86.8}Ni_{8.6}Si_{4.6}$ alloy, respectively (this study); black dash-dotted lines: hcp-Fe (this study) [*Murphy et al.*, 2013]; and blue and gray dash-dot-dotted lines: hcp-$Fe_{0.85}Si_{0.15}$ and hcp-$Fe_{92}Ni_8$ alloys, respectively [*Lin et al.*, 2003]. The PREM model (crosses) for the inner core is also plotted for comparison [*Dziewonski and Anderson*, 1981]. Vertical ticks are representative errors ($\pm1\sigma$) calculated using standard error propagations.

Gao et al., 2011; *Chen et al.*, 2014; *Prescher et al.*, 2015]. Recent theoretical calculations on hcp-Fe have shown that the V_S of hcp-Fe significantly decreases with increasing temperature at core pressures such that the Poisson's ratio approximately increases 65% and 37% from 0 K to 6000 K at 10.43 and 12.52 g/cm^3, respectively (Figure 5b) [*Sha and Cohen*, 2010]. On the other hand, analysis of the shock wave measurements showed that the Poisson's ratio of hcp-Fe can reach to approximately 0.40 at relevant conditions of the core [*Duffy and Ahrens*, 1992], indicating that other factors such as the addition of light element(s) and/or the presence of partially melted materials are still needed to account for the very high Poisson's ratio of the inner core [e.g., *Duffy and Ahrens*, 1992; *Singh et al.*, 2000]. The strong high-temperature effect on Poisson's ratio has also been observed for iron carbides (Fe_3C and Fe_7C_3) from high *P-T* NRIXS experiments (Figure 5a) [*Gao et al.*, 2011; *Prescher et al.*, 2015]. The increased Poisson's ratio at high temperatures mostly results from the considerable reduction in V_S of hcp-Fe and Fe-rich alloys, while V_P is not as strongly reduced at high temperatures [e.g., *Lin et al.*, 2005; *Sha and Cohen*, 2010]. Therefore, high-temperature effect should be considered for the Poisson's ratio and V_S of hcp-Fe and Fe-rich alloys at inner core conditions.

4.4. Seismic Heterogeneity Ratios of hcp-Fe and Fe-Ni-Si Alloys

We have evaluated representative seismic heterogeneity ratios of hcp-Fe and Fe-Ni-Si alloys at high pressures and room temperature, including the ratio of relative density to compressional velocity heterogeneity ($R_{\rho/P} = d\ln\rho/d\ln V_P$), the ratio of relative density to shear velocity heterogeneity ($R_{\rho/S} = d\ln\rho/d\ln V_S$), and the ratio of relative compressional to shear velocity heterogeneity ($R_{P/S} = d\ln V_P/d\ln V_S$) (Figure 6). To the best of our knowledge, this is the first mineral physics attempt to evaluate these seismic heterogeneity ratios of hcp-Fe and Fe-Ni-Si alloy at pressures relevant to the Earth's core. Analysis of these ratios shows that the addition of either Si or Ni has a relatively minor effect on these ratios at high pressures and 300 K. Comparison of the seismic heterogeneity ratios of hcp-$Fe_{86.8}Ni_{8.6}Si_{4.6}$ to pure hcp-Fe at 300 K shows that the combined effects of 9.0 wt % Ni and 2.3 wt % Si increases $d\ln\rho/d\ln V_P$ from approximately 0.8 (±0.1) to 1.0 (±0.1), decreases $d\ln\rho/d\ln V_S$ from approximately 1.0 (±0.2) to 0.8 (±0.2), and drops $d\ln V_P/d\ln V_S$ from approximately 1.2 (±0.2) to 0.7 (±0.2), making them better match PREM values at approximately 1.2, 0.55, and 0.45, respectively. We should note, however, that our estimated seismic heterogeneity ratios carry significantly large uncertainties that are about 15% for $d\ln\rho/d\ln V_P$, 20% $d\ln\rho/d\ln V_S$, and 20% $d\ln V_P/d\ln V_S$ (Figure 6); these large uncertainties are due to the difficulties in measuring the velocity-density relations of Fe and Fe-rich alloys precisely at the inner core

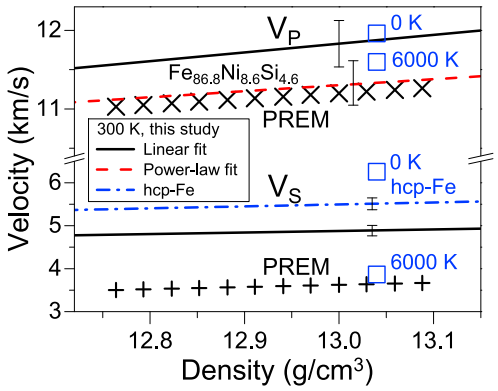

Figure 7. Sound velocity-density relations of hcp-Fe and $Fe_{86.8}Ni_{8.6}Si_{4.6}$ alloy as a function of density. The density-velocity profile from the PREM model (crosses) is also plotted for comparison [*Dziewonski and Anderson*, 1981]. Solid and dashed lines: linear and power law fits for hcp-$Fe_{86.8}Ni_{8.6}Si_{4.6}$ at 300 K, respectively (this study); dash-dotted line: the V_S of hcp-Fe at 300 K (this study) [*Murphy et al.*, 2013]; squares: hcp-Fe at 0 K and 6000 K [*Steinle-Neumann et al.*, 2001]; and vertical ticks: representative errors ($\pm 1\sigma$) calculated using standard error propagations. For comparison with PREM, the density for ^{57}Fe-enriched samples have been converted using the corresponding natural isotopic compositions with 2% ^{57}Fe [*Hu et al.*, 2003; *Sturhahn and Jackson*, 2007].

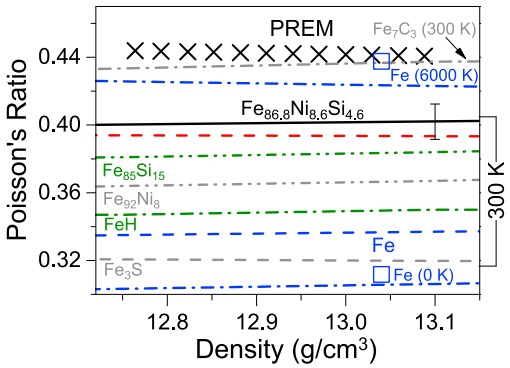

Figure 8. Poisson's ratio of hcp-Fe and Fe-rich alloys as a function of density. The density range corresponds to that in the inner core. The Poisson's ratio of the inner core from the PREM model (crosses) is also plotted for comparison (Dziewonski and Anderson, 1981). Black and red line: the ν of hcp-$Fe_{86.8}Ni_{8.6}Si_{4.6}$ alloy calculated from the linear and power law fits of V_P–ρ at 300 K, respectively (this study); blue dashed line: hcp-Fe at 300 K (this study); blue dash-dotted lines: hcp-Fe at 0 K and 6000 K estimated from theoretical calculations [*Sha and Cohen*, 2010]; squares: theoretical calculations for hcp-Fe at 0 K and 6000 K [*Steinle-Neumann et al.*, 2001]; gray dash-dotted line: orthorhombic Fe_7C_3 at 300 K [*Prescher et al.*, 2015]; olive and gray dash-dot-dotted line: hcp-$Fe_{85}Si_{15}$ and hcp-$Fe_{92}Ni_8$ alloy at 300 K, respectively [*Lin et al.*, 2003]; blue dash-dot-dotted line: Fe-H alloy at 300 K [*Mao et al.*, 2004; *Shibazaki et al.*, 2012]; and gray dashed line: Fe_3S at 300 K [*Lin et al.*, 2004; *Kamada et al.*, 2014].

conditions. The extrapolated V_P-ρ profiles of hcp-Fe at 300 K, 700 K, and 6000 K display a similar trend under inner core pressures, implying that the high-temperature effects on the $R_{\rho/P}$, $R_{\rho/S}$, and $R_{P/S}$ ratios of hcp-Fe and Fe-Ni-Si alloys might be weak probably due to a smaller thermal expansion of Fe-rich alloys in the Earth's core [*Mao et al.*, 2012]. Although these ratios have been extensively discussed to interpret the seismic heterogeneities in the Earth's mantle [e.g., *Simmons et al.*, 2009; *Wu and Wentzcovitch*, 2014], the use of these ratios in deciphering the presence of seismic heterogeneities in the Earth's inner core remains challenging due to the extreme remoteness of the inner core with low probabilities in seismic traversals [*Wang et al.*, 2015]. Our results here thus provide constraints for future high-resolution seismic studies of the inner core that may one day be able to use these ratios to reveal detailed compositional, structural, and/or dynamic heterogeneities of the region [*Deuss*, 2014].

4.5. Fe-Ni-Si Alloy in the Earth's Inner Core

In order to reliably constrain the composition and seismic structures of the Earth's inner core, physical properties of Fe-Ni alloyed with light element(s) at relevant high *P-T* conditions should match all seismic observations of the region including V_P, V_S, ρ, υ, and aforementioned seismic heterogeneity ratios, instead of satisfying one constraint while neglecting others. To decipher whether or not hcp-Fe alloyed with Ni and Si can satisfy these multiple geophysical constraints, the V_P-ρ, V_S-ρ, and Poisson's ratio profiles of hcp-Fe and Fe-Ni-Si alloys have been extrapolated to the pressures of the inner core (Figures 7 and 8). The V_P-ρ of the naturally isotopic hcp-$Fe_{86.8}Ni_{8.6}Si_{4.6}$ composition was extrapolated to the inner core density by a linear function and a power law relation, respectively (Figure 7). The V_P of the alloy from the linear fit at 300 K is approximately 4% higher than that of the inner core at a given density (e.g., PREM), while the V_P of the alloy from the power law fit at 300 K matches well with the values of PREM (Figure 7). The V_S of hcp-Fe and $Fe_{86.8}Ni_{8.6}Si_{4.6}$ alloy extrapolated at 300 K displays much greater values than that of PREM, by approximately 50% and 35%, respectively. Among all the Fe-rich alloys, the hcp-$Fe_{86.8}Ni_{8.6}Si_{4.6}$ shows a high Poisson's ratio of about 0.4 at 300 K, which is lower than the ratio of Fe_7C_3 (Figure 8). It is worthwhile to point out that the V_P of Fe_7C_3 is ~13 km/s in the inner core as

extrapolated from *Prescher et al*. [2015] and thus ~15% higher than PREM and that the high temperatures seem to raise up the Poisson's ratio of Fe_7C_3 much greater than that of the inner core, which most likely excludes Fe_7C_3 as the major component of the inner core. On the other hand, since the high temperature (e.g., 6000 K) is expected to greatly reduce the V_S of the Fe-rich Fe-Ni-Si alloy but slightly decrease the V_P, it is conceivable that the Poisson's ratio of the hcp-$Fe_{86.8}Ni_{8.6}Si_{4.6}$ alloy at relevant high *P-T* conditions of the inner core will be enhanced to a value that better matches seismic observations (e.g., PREM). We note that our experimental results on the hcp-$Fe_{86.8}Ni_{8.6}Si_{4.6}$ alloy at 300 K were not extrapolated to high temperatures relevant to inner core conditions because of the large uncertainty of the high-temperature effects on seismic parameters of the alloys among previous experimental and theoretical results. Future high-quality data sets of the Fe alloys at high *P-T* conditions are critically needed to eventually provide reliable experimental constraints in order to solve these longstanding issues regarding the geophysics and geochemistry of the Earth's core.

The use of the multiple geophysical constraints reported here provides a convincing argument for the Fe-Ni-Si alloy in the hcp structure as a candidate major component of the Earth's inner core and shows that the addition of Ni and Si can significantly reduce the V_S of hcp-Fe, together with the high-temperature effect on V_S, thus accounting for the anomalously high υ in the Earth's inner core. It remains to be further understood as to how the existence of hcp-Fe alloyed with Ni and Si in the Earth's inner core can result in the presence of seismic heterogeneities in this region, which in turn may help us understand the thermal and compositional evolution of the inner core. Moreover, the accurate determination of silicon abundance in the core needs more critical constraints on the temperature dependence of seismic parameters of hcp-Fe and Fe-Ni-Si alloys at high pressures from future studies, together with geochemical constraints on the distribution of siderophile elements during the metal-silicate differentiation in the primitive Earth [*Badro et al*., 2015].

Acknowledgments

We acknowledge D. Fan, W. Bi, E.E. Alp, and J. Wu for their experimental assistance and constructive discussions. We thank J. Beam for assisting with editing the manuscript. J.F. Lin acknowledges support from the U.S. National Science Foundation (EAR-0838221 and EAR1446946) and the Center for High Pressure Science and Technology Advanced Research (HPSTAR). HPSTAR is supported by NSAF (grant U1530402). We acknowledge XOR3 of the APS for the use of the inelastic X-ray scattering facilities and GSECARS and HPCAT of the APS for use of the diffraction and ruby facilities. This research used resources of the Advanced Photon Source, a U.S. Department of Energy (DOE) Office of Science User Facility operated for the DOE Office of Science by Argonne National Laboratory under contract DE-AC02-06CH11357. Data used in this study are available from Jung-Fu Lin (Email: afu@jsg.utexas.edu) and Jin Liu (Email: jinliu@utexas.edu) upon request.

References

Alatas, A., B. M. Leu, J. Zhao, H. Yavaş, T. S. Toellner, and E. E. Alp (2011), Improved focusing capability for inelastic X-ray spectrometer at 3-ID of the APS: A combination of toroidal and Kirkpatrick-Baez (KB) mirrors, *Nucl. Instrum. Methods Phys. Res., Sect. A*, *649*(1), 166–168, doi:10.1016/j.nima.2010.11.068.

Antonangeli, D., and E. Ohtani (2015), Sound velocity of hcp-Fe at high pressure: Experimental constraints, extrapolations and comparison with seismic models, *Prog. Earth Planet. Sci.*, *2*(1), 1–11, doi:10.1186/s40645-015-0034-9.

Antonangeli, D., J. Siebert, J. Badro, D. L. Farber, G. Fiquet, G. Morard, and F. J. Ryerson (2010), Composition of the Earth's inner core from high-pressure sound velocity measurements in Fe–Ni–Si alloys, *Earth Planet. Sci. Lett.*, *295*(1–2), 292–296, doi:10.1016/j.epsl.2010.04.018.

Antonangeli, D., T. Komabayashi, F. Occelli, E. Borissenko, A. C. Walters, G. Fiquet, and Y. Fei (2012), Simultaneous sound velocity and density measurements of hcp iron up to 93 GPa and 1100 K: An experimental test of the Birch's law at high temperature, *Earth Planet. Sci. Lett.*, *331–332*, 210–214, doi:10.1016/j.epsl.2012.03.024.

Asanuma, H., E. Ohtani, T. Sakai, H. Terasaki, S. Kamada, N. Hirao, and Y. Ohishi (2011), Static compression of $Fe_{0.83}Ni_{0.09}Si_{0.08}$ alloy to 374 GPa and $Fe_{0.93}Si_{0.07}$ alloy to 252 GPa: Implications for the Earth's inner core, *Earth Planet. Sci. Lett.*, *310*(1–2), 113–118, doi:10.1016/j.epsl.2011.06.034.

Badro, J., G. Fiquet, F. Guyot, E. Gregoryanz, F. Occelli, D. Antonangeli, and M. d'Astuto (2007), Effect of light elements on the sound velocities in solid iron: Implications for the composition of Earth's core, *Earth Planet. Sci. Lett.*, *254*(1–2), 233–238, doi:10.1016/j.epsl.2006.11.025.

Badro, J., J. P. Brodholt, H. Piet, J. Siebert, and F. J. Ryerson (2015), Core formation and core composition from coupled geochemical and geophysical constraints, *Proc. Natl. Acad. Sci. U.S.A.*, *112*(40), 12,310–12,314, doi:10.1073/pnas.1505672112.

Belonoshko, A. B., R. Ahuja, and B. Johansson (2003), Stability of the body-centred-cubic phase of iron in the Earth's inner core, *Nature*, *424*(6952), 1032–1034, doi:10.1038/nature01954.

Birch, F. (1952), Elasticity and constitution of the Earth's interior, *J. Geophys. Res.*, *57*, 227–286, doi:10.1029/JZ057i002p00227.

Chen, B., et al. (2014), Hidden carbon in Earth's inner core revealed by shear softening in dense Fe_7C_3, *Proc. Natl. Acad. Sci. U.S.A.*, *111*(50), 17,755–17,758, doi:10.1073/pnas.1411154111.

Decremps, F., D. Antonangeli, M. Gauthier, S. Ayrinhac, M. Morand, G. L. Marchand, F. Bergame, and J. Philippe (2014), Sound velocity of iron up to 152 GPa by picosecond acoustics in diamond anvil cell, *Geophys. Res. Lett.*, *41*, 1459–1464, doi:10.1002/2013GL058859.

Deuss, A. (2014), Heterogeneity and anisotropy of Earth's inner core, *Annu. Rev. Earth Planet. Sci.*, *42*(1), 103–126, doi:10.1146/annurev-earth-060313-054658.

Dewaele, A., P. Loubeyre, F. Occelli, M. Mezouar, P. I. Dorogokupets, and M. Torrent (2006), Quasihydrostatic equation of state of iron above 2 Mbar, *Phys. Rev. Lett.*, *97*(21), 215504, doi:10.1103/PhysRevLett.97.215504.

Dubrovinsky, L., and J.-F. Lin (2009), Mineral physics quest to the Earth's core, *Eos Trans. AGU*, *90*(3), 21–22, doi:10.1029/2009EO030001.

Duffy, T. S., and T. J. Ahrens (1992), Hugoniot sound velocities in metals with applications to the Earth's inner core, in *High-Pressure Research: Application to Earth And Planetary Sciences*, edited by Y. Syono and M. H. Manghnani, pp. 353–361, AGU, Washington, D. C.

Dziewonski, A. M., and D. L. Anderson (1981), Preliminary reference Earth model, *Phys. Earth Planet Int.*, *25*, 297–356.

Fei, Y., A. Ricolleau, M. Frank, K. Mibe, G. Shen, and V. Prakapenka (2007), Toward an internally consistent pressure scale, *Proc. Natl. Acad. Sci. U.S.A.*, *104*(22), 9182–9186, doi:10.1073/pnas.0609013104.

Fiquet, G., J. Badro, F. Guyot, H. Requardt, and M. Krisch (2001), Sound velocities in iron to 110 gigapascals, *Science*, *291*(5503), 468–471, doi:10.1126/science.291.5503.468.

Gao, L., B. Chen, J. Zhao, E. E. Alp, W. Sturhahn, and J. Li (2011), Effect of temperature on sound velocities of compressed Fe_3C, a candidate component of the Earth's inner core, *Earth Planet. Sci. Lett.*, *309*(3–4), 213–220, doi:10.1016/j.epsl.2011.06.037.

Gessmann, C. K., B. J. Wood, D. C. Rubie, and M. R. Kilburn (2001), Solubility of silicon in liquid metal at high pressure: Implications for the composition of the Earth's core, *Earth Planet. Sci. Lett.*, *184*(2), 367–376, doi:10.1016/S0012-821X(00)00325-3.

Gleason, A. E., W. L. Mao, and J. Y. Zhao (2013), Sound velocities for hexagonally close-packed iron compressed hydrostatically to 136 GPa from phonon density of states, *Geophys. Res. Lett.*, *40*, 2983–2987, doi:10.1002/grl.50588.
Hill, R. (1952), The elastic behaviour of a crystalline aggregate, *Proc. Phys. Soc. A*, *65*(5), 349–354, doi:10.1088/0370-1298/65/5/307.
Hirose, K., S. Labrosse, and J. Hernlund (2013), Composition and state of the core, *Annu. Rev. Earth Planet. Sci.*, *41*(1), 657–691, doi:10.1146/annurev-earth-050212-124007.
Hu, M., W. Sturhahn, T. S. Toellner, P. D. Mannheim, D. E. Brown, J. Zhao, and E. E. Alp (2003), Measuring velocity of sound with nuclear resonant inelastic x-ray scattering, *Phys. Rev. B*, *67*, 094304, doi:10.1103/PhysRevB.67.094304.
Kamada, S., et al. (2014), The sound velocity measurements of Fe_3S, *Am. Mineral.*, *99*(1), 98–101, doi:10.2138/am.2014.4463.
Kantor, A. P., S. D. Jacobsen, I. Y. Kantor, L. S. Dubrovinsky, C. A. McCammon, H. J. Reichmann, and I. N. Goncharenko (2004), Pressure-induced magnetization in FeO: Evidence from elasticity and Möossbauer spectroscopy, *Phys. Rev. Lett.*, *93*(21), 215502, doi:10.1103/PhysRevLett.93.215502.
Li, J., and Y. Fei (2014), Experimental constraints on core composition, in *Treatise on Geochemistry*, 2nd ed., edited by H. D. Holland and K. K. Turekian, pp. 527–557, Elsevier, Oxford.
Lin, J.-F., D. L. Heinz, A. J. Campbell, J. M. Devine, and G. Shen (2002), Iron-silicon alloy in Earth's core?, *Science*, *295*(5553), 313–315, doi:10.1126/science.1066932.
Lin, J.-F., V. V. Struzhkin, W. Sturhahn, E. Huang, J. Zhao, M. Y. Hu, E. E. Alp, H.-k. Mao, N. Boctor, and R. J. Hemley (2003), Sound velocities of iron-nickel and iron-silicon alloys at high pressures, *Geophys. Res. Lett.*, *30*(21), 2112, doi:10.1029/2003GL018405.
Lin, J.-F., Y. Fei, W. Sturhahn, J. Zhao, H.-K. Mao, and R. J. Hemley (2004), Magnetic transition and sound velocities of Fe_3S at high pressure: Implications for Earth and planetary cores, *Earth Planet. Sci. Lett.*, *226*(1–2), 33–40, doi:10.1016/j.epsl.2004.07.018.
Lin, J.-F., W. Sturhahn, J. Zhao, G. Shen, H.-k. Mao, and R. J. Hemley (2005), Sound velocities of hot dense iron: Birch's law revisited, *Science*, *308*(5730), 1892–1894, doi:10.1126/science.1111724.
Lin, J.-F., Z. Mao, H. Yavaş, J. Zhao, and L. Dubrovinsky (2010), Shear wave anisotropy of textured hcp-Fe in the Earth's inner core, *Earth Planet. Sci. Lett.*, *298*(3–4), 361–366, doi:10.1016/j.epsl.2010.08.006.
Lin, J.-F., J. Wu, J. Zhu, Z. Mao, A. H. Said, B. M. Leu, J. Cheng, Y. Uwatoko, C. Jin, and J. Zhou (2014), Abnormal elastic and vibrational behaviors of magnetite at high pressures, *Sci. Rep.*, *4*, 6282, doi:10.1038/srep06282.
Liu, J., J.-F. Lin, A. Alatas, and W. Bi (2014), Sound velocities of bcc-Fe and $Fe_{0.85}Si_{0.15}$ alloy at high pressure and temperature, *Phys. Earth Planet. Inter.*, *233*, 24–32, doi:10.1016/j.pepi.2014.05.008.
Mao, H.-K., Y. Wu, L. C. Chen, J. F. Shu, and A. P. Jephcoat (1990), Static compression of iron to 300 GPa and $Fe_{0.8}Ni_{0.2}$ alloy to 260 GPa: Implications for composition of the core, *J. Geophys. Res.*, *95*(B13), 21,737–21,742, doi:10.1029/JB095iB13p21737.
Mao, H.-K., J. Shu, G. Shen, R. J. Hemley, B. Li, and A. K. Singh (1998), Elasticity and rheology of iron above 220 GPa and the nature of the Earth's inner core, *Nature*, *396*(6713), 741–743, doi:10.1038/396741a0.
Mao, H.-K., et al. (2001), Phonon density of states of iron up to 153 gigapascals, *Science*, *292*(5518), 914–916, doi:10.1126/science.1057670.
Mao, W. L., W. Sturhahn, D. L. Heinz, H.-K. Mao, J. Shu, and R. J. Hemley (2004), Nuclear resonant X-ray scattering of iron hydride at high pressure, *Geophys. Res. Lett.*, *31*, L15618, doi:10.1029/2004GL020541.
Mao, Z., J.-F. Lin, J. Liu, A. Alatas, L. Gao, J. Zhao, and H.-K. Mao (2012), Sound velocities of Fe and Fe-Si alloy in the Earth's core, *Proc. Natl. Acad. Sci. U.S.A.*, *109*(26), 10,239–10,244, doi:10.1073/pnas.1207086109.
Martorell, B., J. Brodholt, I. G. Wood, and L. Vočadlo (2013), The effect of nickel on the properties of iron at the conditions of Earth's inner core: Ab initio calculations of seismic wave velocities of Fe–Ni alloys, *Earth Planet. Sci. Lett.*, *365*, 143–151, doi:10.1016/j.epsl.2013.01.007.
Murphy, C. A., J. M. Jackson, and W. Sturhahn (2013), Experimental constraints on the thermodynamics and sound velocities of hcp-Fe to core pressures, *J. Geophys. Res. Solid Earth*, *118*, 1999–2016, doi:10.1002/jgrb.50166.
Nguyen, J. H., and N. C. Holmes (2004), Melting of iron at the physical conditions of the Earth's core, *Nature*, *427*(6972), 339–342, doi:10.1038/nature02248.
Ohtani, E., Y. Shibazaki, T. Sakai, K. Mibe, H. Fukui, S. Kamada, T. Sakamaki, Y. Seto, S. Tsutsui, and A. Q. R. Baron (2013), Sound velocity of hexagonal close-packed iron up to core pressures, *Geophys. Res. Lett.*, *40*, 5089–5094, doi:10.1002/grl.50992.
Prescher, C., et al. (2015), High Poisson's ratio of Earth's inner core explained by carbon alloying, *Nat. Geosci.*, *8*, 220–223, doi:10.1038/ngeo2370.
Sakai, T., E. Ohtani, N. Hirao, and Y. Ohishi (2011), Stability field of the hcp-structure for Fe, Fe-Ni, and Fe-Ni-Si alloys up to 3 Mbar, *Geophys. Res. Lett.*, *38*, L09302, doi:10.1029/2011GL047178.
Seagle, C. T., E. Cottrell, Y. Fei, D. R. Hummer, and V. B. Prakapenka (2013), Electrical and thermal transport properties of iron and iron-silicon alloy at high pressure, *Geophys. Res. Lett.*, *40*, 5377–5381, doi:10.1002/2013GL057930.
Sha, X., and R. E. Cohen (2010), Elastic isotropy of ε-Fe under Earth's core conditions, *Geophys. Res. Lett.*, *37*, L10302, doi:10.1029/2009GL042224.
Shibazaki, Y., et al. (2012), Sound velocity measurements in dhcp-FeH up to 70 GPa with inelastic X-ray scattering: Implications for the composition of the Earth's core, *Earth Planet. Sci. Lett.*, *313–314*, 79–85, doi:10.1016/j.epsl.2011.11.002.
Siebert, J., J. Badro, D. Antonangeli, and F. J. Ryerson (2013), Terrestrial accretion under oxidizing conditions, *Science*, *339*, 1194–1197, doi:10.1126/science.1227923.
Simmons, N. A., A. M. Forte, and S. P. Grand (2009), Joint seismic, geodynamic and mineral physical constraints on three-dimensional mantle heterogeneity: Implications for the relative importance of thermal versus compositional heterogeneity, *Geophys. J. Int.*, *177*(3), 1284–1304, doi:10.1111/j.1365-246X.2009.04133.x.
Singh, S. C., M. A. J. Taylor, and J. P. Montagner (2000), On the presence of liquid in Earth's inner core, *Science*, *287*(5462), 2471–2474, doi:10.1126/science.287.5462.2471.
Steinle-Neumann, G., L. Stixrude, R. E. Cohen, and O. Gülseren (2001), Elasticity of iron at the temperature of the Earth's inner core, *Nature*, *413*(6851), 57–60, doi:10.1038/35092536.
Sturhahn, W. (2000), CONUSS and PHOENIX: Evaluation of nuclear resonant scattering data, *Hyperfine Interact.*, *125*(1–4), 149–172, doi:10.1023/A:1012681503686.
Sturhahn, W., and J. M. Jackson (2007), Geophysical applications of nuclear resonant spectroscopy, *Geol. Soc. Am. Spec. Pap.*, *421*, 157–174, doi:10.1130/2007.2421(09).
Tateno, S., Y. Kuwayama, K. Hirose, and Y. Ohishi (2015), The structure of Fe–Si alloy in Earth's inner core, *Earth Planet. Sci. Lett.*, *418*, 11–19, doi:10.1016/j.epsl.2015.02.008.
Toellner, T. S., A. Alatas, and A. H. Said (2011), Six-reflection meV-monochromator for synchrotron radiation, *J. Synchrotron Radiat.*, *18*(4), 605–611, doi:10.1107/S0909049511017535.
Vočadlo, L., D. P. Dobson, and I. G. Wood (2009), Ab initio calculations of the elasticity of hcp-Fe as a function of temperature at inner-core pressure, *Earth Planet. Sci. Lett.*, *288*(3–4), 534–538, doi:10.1016/j.epsl.2009.10.015.

Wang, T., X. Song, and H. H. Xia (2015), Equatorial anisotropy in the inner part of Earth's inner core from autocorrelation of earthquake coda, *Nat. Geosci.*, *8*(3), 224–227, doi:10.1038/ngeo2354.

Wenk, H.-R., S. Matthies, R. J. Hemley, H.-K. Mao, and J. Shu (2000), The plastic deformation of iron at pressures of the Earth's inner core, *Nature*, *405*(6790), 1044–1047, doi:10.1038/35016558.

Wu, Z., and R. M. Wentzcovitch (2014), Spin crossover in ferropericlase and velocity heterogeneities in the lower mantle, *Proc. Natl. Acad. Sci. U.S.A.*, *111*(29), 10,468–10,472, doi:10.1073/pnas.1322427111.

Zhang, Y., T. Sekine, H. He, Y. Yu, F. Liu, and M. Zhang (2014), Shock compression of Fe-Ni-Si system to 280 GPa: Implications for the composition of the Earth's outer core, *Geophys. Res. Lett.*, *41*, 4554–4559, doi:10.1002/2014GL060670.

Zhao, J., W. Sturhahn, J.-F. Lin, G. Shen, E. E. Alp, and H.-K. Mao (2004), Nuclear resonant scattering at high pressure and high temperature, *High Pressure Res.*, *24*(4), 447–457, doi:10.1080/08957950412331331727.